STRUCTURAL SCIENCE
CRYSTAL ENGINEERING
MATERIALS

Volume 76 (2020)

Supporting information for article:

0D to 3D Pr^{III} metal–organic networks crystal engineered for optimal iodine adsorption

Faezeh Moghzi, Janet Soleimannejad, Hamid Emadi and Jan Janczak

Contents

Table S1. Hydrogen-bond geometry (Å, º) for I.

D—H···*A*	*D*—H	H···*A*	*D*···*A*	*D*—H···*A*
N4—H4*A*···O7^{i}	0.91	1.94	2.781 (7)	154
N4—H4*B*···O12	0.91	1.86	2.698 (7)	152
N5—H5*A*···O9	0.91	1.90	2.732 (7)	151
N5—H5*B*···O1^{ii}	0.91	2.65	3.270 (7)	126
N5—H5*B*···O8^{ii}	0.91	1.91	2.780 (7)	159
N6—H6*A*···O13	0.91	1.91	2.767 (7)	155
N6—H6*B*···O11^{ii}	0.91	1.89	2.798 (8)	176
C13—H131···O4^{i}	0.99	2.59	3.117 (8)	113
C13—H131···O12^{iii}	0.99	2.53	3.209 (8)	126
C15—H15···O10^{iv}	0.95	2.48	3.317 (8)	146
C16—H162···O12^{iii}	0.99	2.50	3.190 (8)	126
C17—H17···O11^{iv}	0.95	2.55	3.383 (8)	147
C18—H181···O1^{ii}	0.99	2.58	3.095 (8)	112
C18—H181···O9^{v}	0.99	2.45	3.164 (8)	129
C18—H182···O13	0.99	2.63	3.443 (8)	140
C19—H19···O1^{vi}	0.95	2.64	3.496 (8)	151
C20—H202···O9^{v}	0.99	2.53	3.218 (8)	127

Symmetry codes: (i) *x*+1, *y*, *z*; (ii) *x*-1, *y*, *z*; (iii) -*x*+2, -*y*+1, -*z*+1; (iv) *x*, *y*+1, *z*; (v) -*x*, -*y*+1, -*z*; (vi) -*x*+1, -*y*+1, -*z*.

Table S2. Hydrogen-bond geometry (Å, º) for II.

D—H···*A*	*D*—H	H···*A*	*D*···*A*	*D*—H···*A*

O14—H14*A*···O6	1.08 (4)	1.40 (4)	2.471 (3)	173 (3)
O6—H14*A*···O13	1.40 (4)	2.41 (3)	3.215 (3)	112.3 (19)
C25—H25···O3^{i}	0.95	2.59	3.481 (3)	156
O1—H1*A*···O4^{ii}	0.86	2.21	2.711 (2)	118
O1—H1*B*···O3	0.86	1.92	2.713 (2)	154
O2—H2*A*···O12^{iii}	0.85	2.21	2.702 (2)	116
O2—H2*B*···O22	0.85	1.94	2.712 (2)	150
O3—H3*A*···O24^{iv}	0.85	1.99	2.840 (2)	174
O3—H3*B*···O23^{v}	0.85	2.04	2.866 (2)	163
O4—H4*A*···O24	0.85	1.84	2.695 (2)	177
O4—H4*B*···O3^{vi}	0.85	2.11	2.856 (2)	145
O5—H5*A*···O4^{vii}	0.85	2.20	2.976 (3)	150
O5—H5*B*···O11^{viii}	0.85	2.09	2.939 (3)	171
O6—H6*A*···O5	0.85	2.05	2.772 (3)	142
O6—H6*B*···O12^{viii}	0.85	1.81	2.630 (3)	161

Symmetry codes: (i) -*x*+2, *y*+1/2, -*z*+3/2; (ii) -*x*+2, -*y*+2, -*z*+1; (iii) -*x*+1, *y*-1/2, -*z*+3/2; (iv) -*x*+2, *y*-1/2, -*z*+3/2; (v) *x*, *y*, *z*+1; (vi) *x*, *y*, *z*-1; (vii) *x*, *y*-1, *z*+1; (viii) *x*, *y*-1, *z*.

Table S3. Hydrogen-bond geometry (Å, º) for III.

D—H···*A*	*D*—H	H···*A*	*D*···*A*	*D*—H···*A*
N4—H4*N*···O12^{i}	0.88	1.72	2.597 (7)	171
C5—H5···O4^{ii}	0.95	2.31	3.127 (7)	143
C6—H6···O2^{ii}	0.95	2.44	3.207 (7)	138
C15—H14···O1^{iii}	0.95	2.37	2.970 (8)	121
C16—H16···O13^{iv}	0.95	2.56	3.292 (7)	134
C16—H16···O14^{v}	0.95	2.57	3.318 (7)	136
O1*W*—H1*B*···O13^{vi}	0.88	1.90	2.735 (6)	158
O2*W*—H2*A*···O2^{ii}	0.90	2.07	2.712 (6)	127
O2*W*—H2*B*···O12^{vii}	0.90	1.89	2.716 (6)	152
O3*W*—H3*A*···O13	0.89	2.02	2.870 (6)	162
O3*W*—H3*B*···N11^{vii}	0.88	2.01	2.851 (7)	158

Symmetry codes: (i) -*x*+1, -*y*+1, -*z*+1; (ii) -*x*+1/2, *y*+1/2, *z*; (iii) *x*+1/2, *y*, -*z*+3/2; (iv) -*x*+2, *y*-1/2, -*z*+3/2; (v) -*x*+3/2, *y*-1/2, *z*; (vi) *x*-1, *y*, *z*; (vii) -*x*+3/2, *y*+1/2, *z*.

Table S4. Hydrogen-bond geometry (Å, º) for IV.

D—H···*A*	*D*—H	H···*A*	*D*···*A*	*D*—H···*A*
C5—H5···O3^{i}	0.95	2.57	3.121 (4)	118
C6—H6···O13^{i}	0.95	2.50	3.379 (4)	154
C6—H6···O2*W*	0.95	2.59	3.169 (4)	120
C15—H15···O2^{ii}	0.95	2.49	3.040 (4)	117
C16—H16···O2^{ii}	0.95	2.30	2.941 (4)	124
O1*W*—H1*A*···O4*W*	0.88	1.92	2.742 (4)	156
O1*W*—H1*B*···O4*W*^{iii}	0.88	2.10	2.962 (4)	165
O2*W*—H2*A*···O12	0.87	2.50	3.031 (4)	120
O2*W*—H2*A*···O1*W*^{iv}	0.87	2.44	3.242 (4)	153
O2*W*—H2*A*···O4*W*^{i}	0.87	2.55	3.019 (4)	115
O2*W*—H2*B*···O4^{v}	0.87	1.95	2.751 (4)	152
O3*W*—H3*A*···O12^{iv}	0.87	2.12	2.731 (4)	127
O3*W*—H3*B*···O2^{v}	0.87	1.89	2.618 (4)	140

Symmetry codes: (i) *x*+1, *y*, *z*; (ii) *x*+1/2, -*y*+3/2, *z*-1/2; (iii) -*x*, -*y*+1, -*z*+1; (iv) -*x*+1, -*y*+1, -*z*+1; (v) *x*+1/2, -*y*+3/2, *z*+1/2.

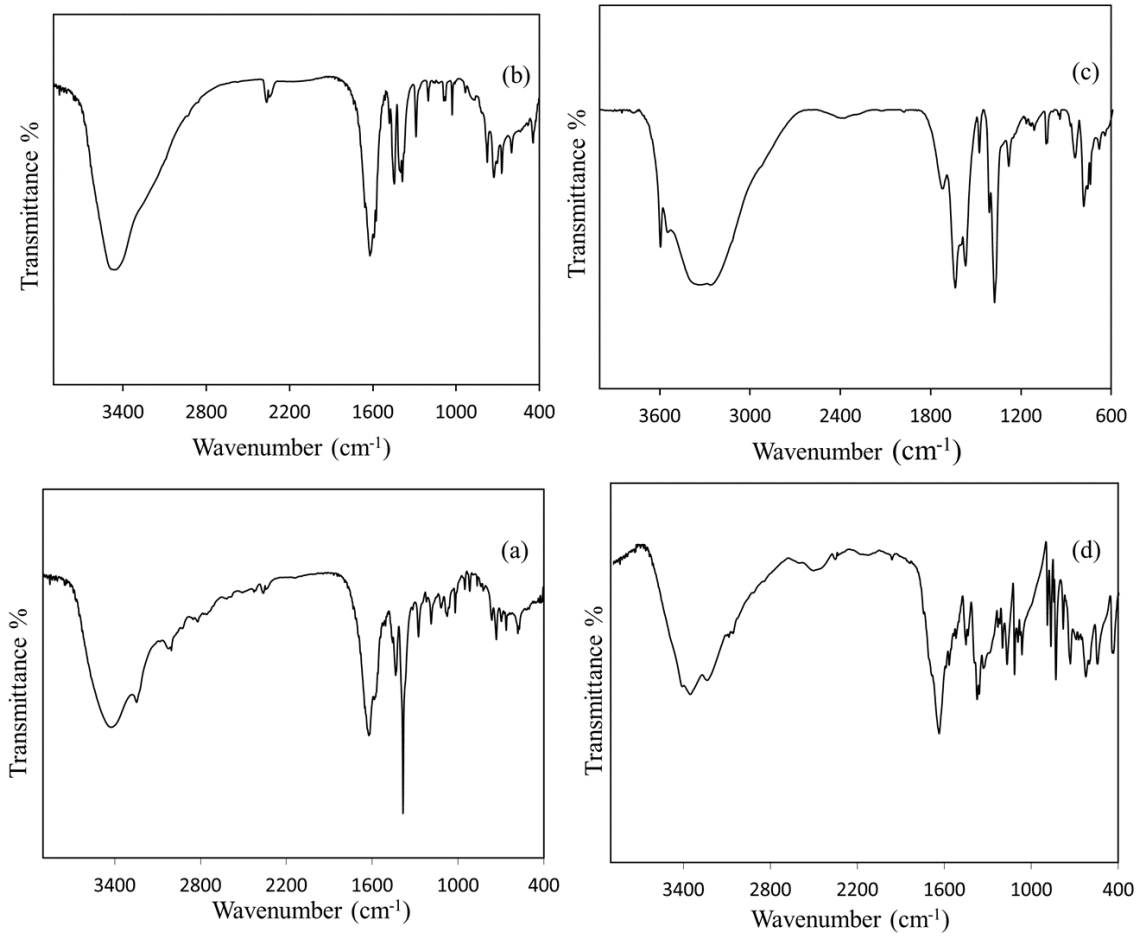

Figure S1. FT-IR Spectra of (a) I, (b) II, (c) III and (d) IV.

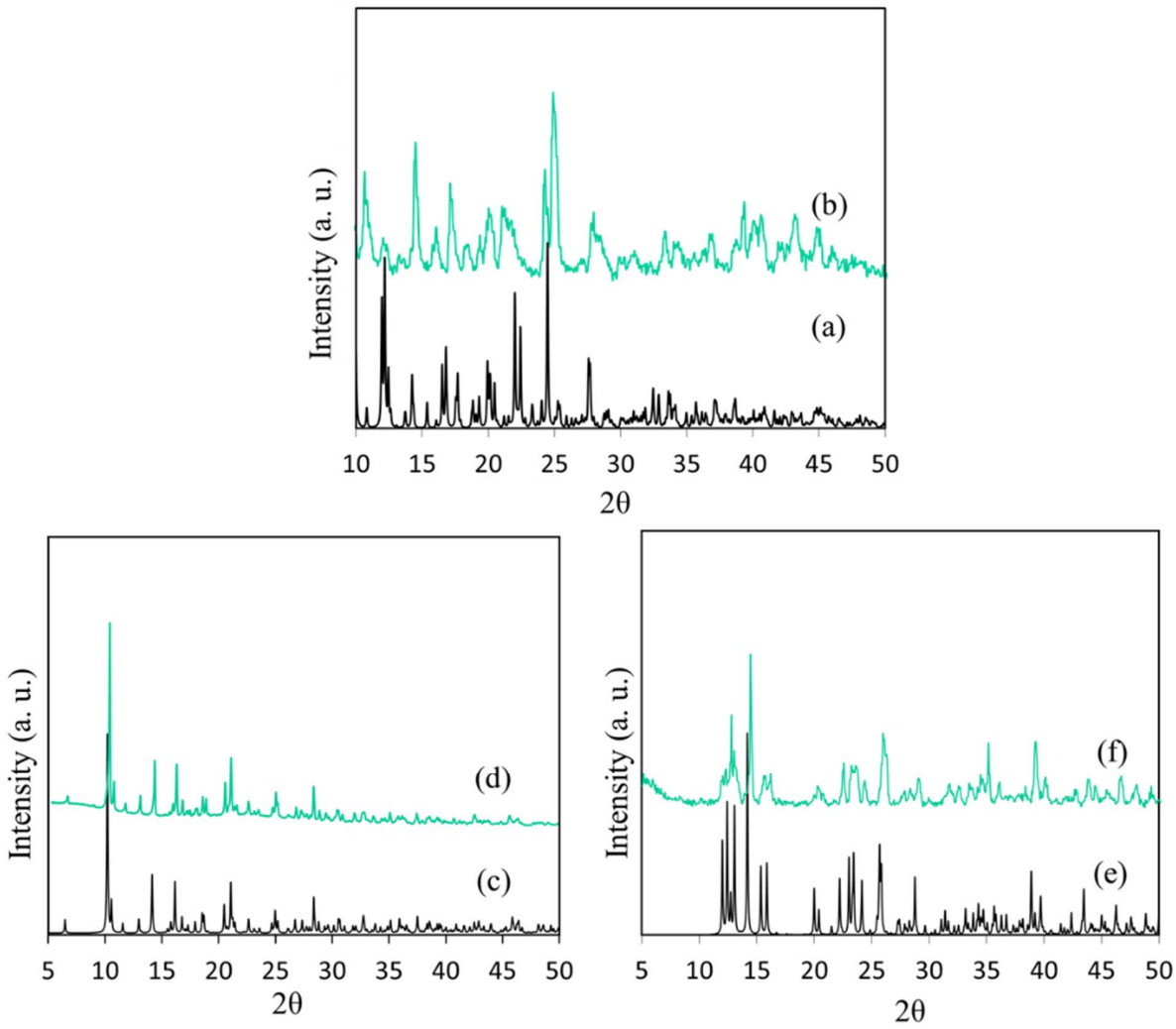
Intensity (a. u.)
(b)
(a)
10 15 20 25 30 35 40 45 50
2θ
Intensity (a. u.)
(d)
(c)
5 10 15 20 25 30 35 40 45 50
2θ
Intensity (a. u.)
(f)
(e)
5 10 15 20 25 30 35 40 45 50
2θ

Figure S2. (a) Simulated PXRD pattern based on single crystal X-ray data of I, (b) XRD patterns of bulk crystals of I prepared in ambient conditions, (c) Simulated XRD pattern based on single crystal X-ray data of II, (d) XRD patterns of bulk crystals of II prepared in ambient conditions, (e) Simulated XRD pattern based on single crystal X-ray data of III, (f) XRD patterns of bulk crystals of III prepared in ambient conditions.

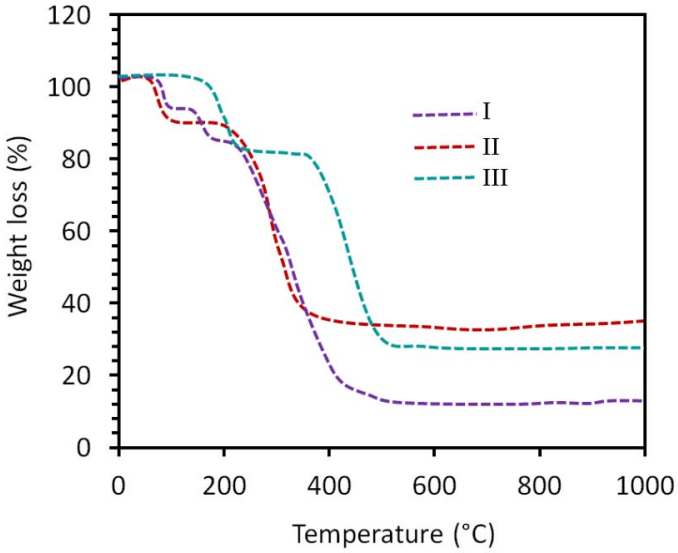

Figure S3. Thermal gravimetery analysis of I, II, III.

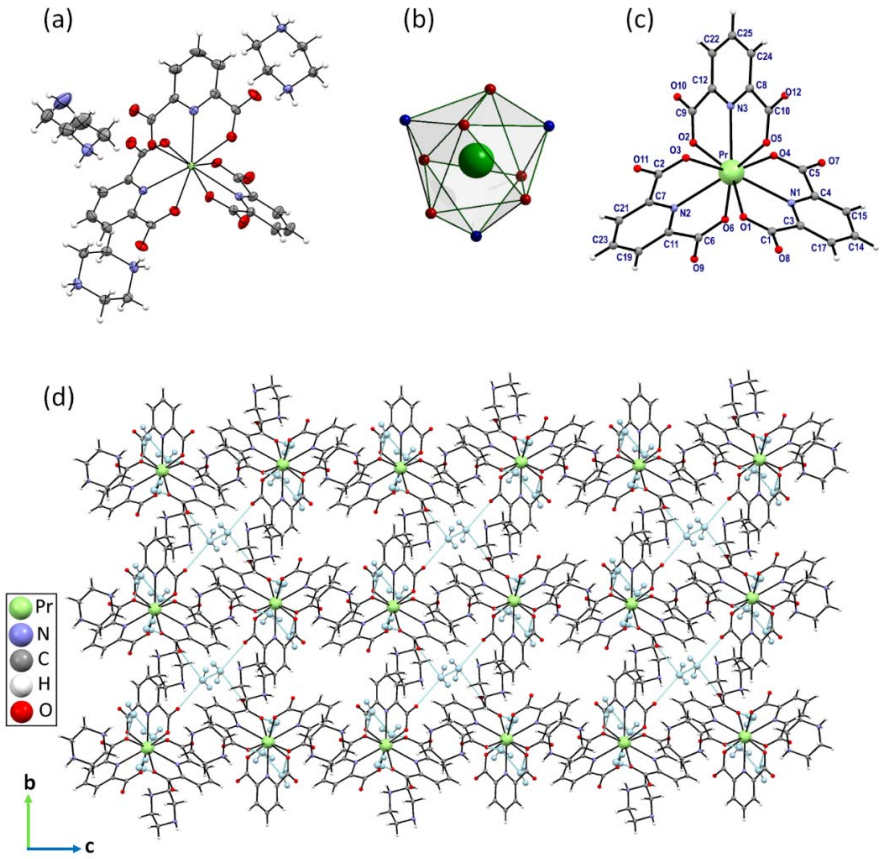

Figure S4. (a) Molecular structure of I, (b) Coordination polyhedron of the Pr(III) ion in I, (c) Coordination environment of I, and (d) 3D supramolecular architecture of I.

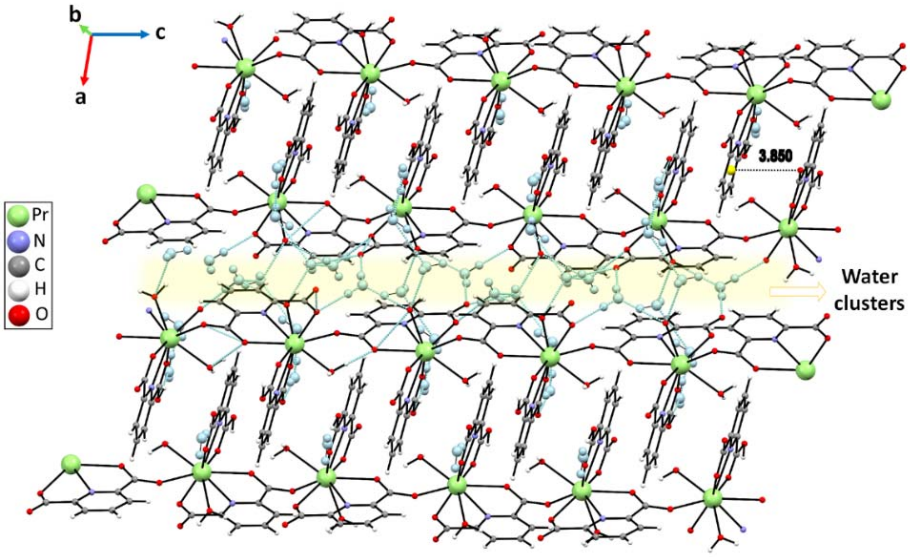

Figure S5. 3D supramolecular architecture of II fromed by hydrogen bonding and π-intraction and water cluster between 1D chains.

Table S5. Comparison of the iodine adsorption capacities of MOFs

Adsorbents	**Iodine uptake (mg/g)**	**Ref.**
MIL-120	125	[1]
MIL-101-NH_2	311	[1]
MIL-53-NH_2	~150	[1]
CAU-1	~300	[1]
MIL-100	~50	[1]
SCMP-1	145	[2]
SCMP-2	184	[2]
Mil-53(Al)$(Al)_{AlO}$	~200	[3]
$[Ca_2(TBAPy)(\mu_2OH_2)_2]\cdot 2DMF$	250	[4]
SINAP-8	473	[5]
MIL-125-NH2@cross-linked chitosan	399	[6]
ZIF-67@CuBi–CO_3-LDH	157	[7]
Uio-67	530	[8]

Cu-BTC@PES	630	[9]
MFM-300(Sc)	1180	[10]
MOF-808	2180	[8]
Compound **IV**	490	This work

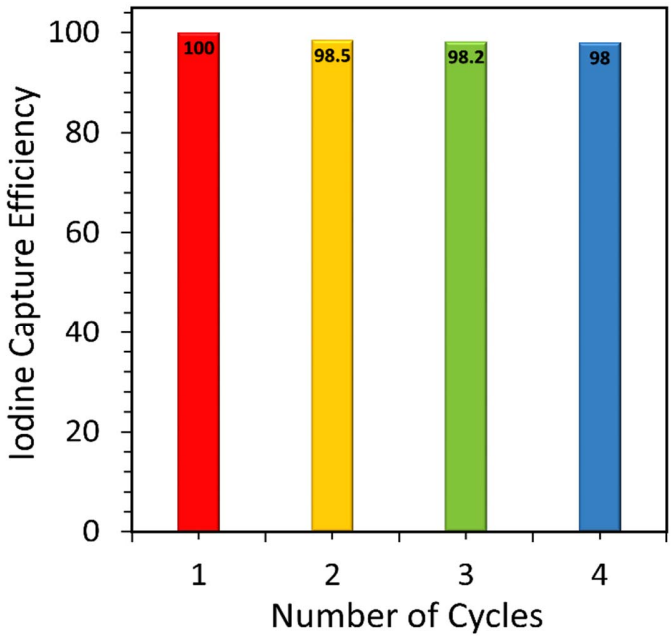

Figure S6. Iodine capture efficiency in IV during four cycles of adsorption-desorption.

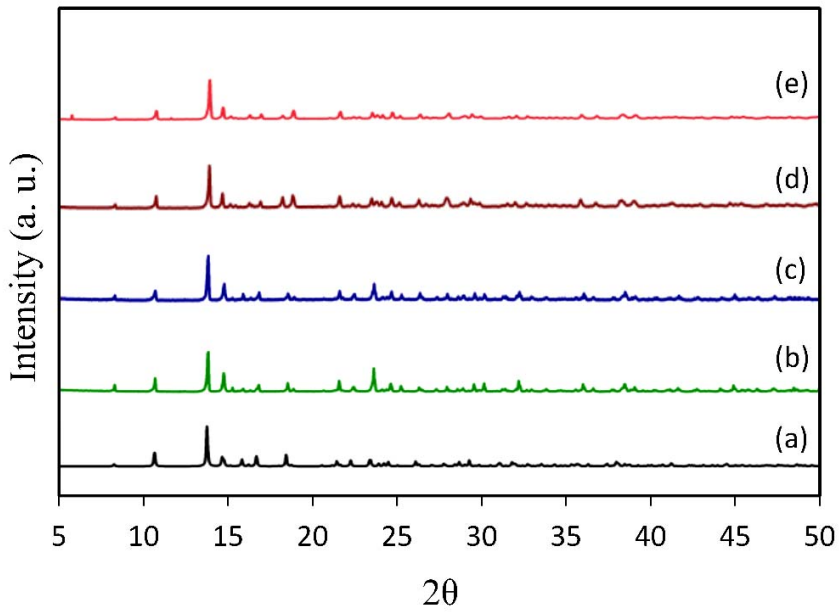

Figure S7. (a) Simulated PXRD pattern based on single crystal X-ray data of IV, (b) PXRD patterns of IV after first cycle of I_2 adsorption, (c) PXRD patterns of IV after first cycle of I_2 desorption, (d) PXRD patterns of IV after second cycle of I_2 adsorption and (e) PXRD patterns of IV after second cycle of I_2 desorption.

Reference

[1] C. Falaise, C. Volkringer, J. Facqueur, T.Bousquet, L. Gasnotb & Thierry Loiseaua, Capture of iodine in highly stable metal–organic frameworks: a systematic study, (2013) *Chemical Communication*, 49, 10320.

[2] *X. Qian, Z-Q. Zhu, H-X. Sun, F. Ren, P. Mu, W. Liang, L. Chen & A. Li,* Capture and reversible storage of volatile iodine by novel conjugated microporous polymers containing thiophene units, (2016) *ACS Applied Materials & Interfaces,* 32, 21063.

[3] L. Feng, R. Chen, Sh. Hou, W. Chen, H. Huang, Y. Wang, Y-N. Wu & F. Li, Common but differentiated flexible MIL-53(Al): role of metal sources in synthetic protocol for tuning the adsorption characteristics, (2019) *Journal of Materials Science,* 54, 6174.

[4] A. Gładysiak, T. N. Nguyen, M. Spodaryk, J-H. Lee, J. B. Neaton, A. Zettel & K. C. Stylianou, Incarceration of iodine in a pyrene-based Metal–Organic Fr,amework, (2019) *Chemistey A European Journal, 25, 501.*

[*5*] Z-J. Li, Z. Yue, Y. Ju, X. Wu, Y. Ren, S. Wang, Y. Li, Z-H. Zhang, X. Guo, J. Lin & J-Q. Wang, Ultrastable thorium metal-organic frameworks for efficient iodine adsorption, (2019) *Inorganic Chemistry,* 59, 4435.

[6] M. El-Shahata, A; E. Abdelhamid, R. M. Abdelhameed, Capture of iodide from wastewater by effective adsorptive membrane synthesized from MIL-125-NH2 and cross-linked chitosan, (2020) *Carbohydrate Polymers*, 231, 115742.

[7] F. Yu, Y. Chen, Y. Wang, C. Liu, J. Qin, Synthesis of metal–organic framework nanocrystals immobilized with 3D flowerlike Cu–Bi-layered double hydroxides for iodine efficient removal, (2020) *Journal of Materials Research*, 3, 299.

[8] P. Chen, X. He, M. Pang, X. Dong, S. Zhao, W. Zhang, Iodine capture using Zr-based metal-organic frameworks (Zr-MOFs): adsorption performance and mechanism, (2020) *ACS Applied Materials & Interfaces*, 12, 18, 20429–20439.

[9] Q. Zhao, L. Zhu, G. Lin, G. Chen, B. Liu, L. Zhang, T. Duan, J. Lei, Controllable synthesis of porous Cu-BTC@polymer composite beads for iodine capture, (2019) *ACS Applied Materials & Interfaces,* 11, 45, 42635–42645.

[10] L. J. Small, R. C. Hill, J. L. Krumhansl, M. E. Schindelholz, Z. Chen, K. W. Chapman, X. Zhang, S. Yang, M. Schröder, T. M. Nenoff, Reversible MOF-based sensors for the electrical detection of iodine gas, (2019) *ACS Applied Materials & Interfaces,* 11, 31, 27982–27988.